

Accurate, robust and reliable calculations of Poisson-Boltzmann binding energies

Duc D. Nguyen,^{†,§} Bao Wang,^{†,§} and Guo-Wei Wei^{*,†,‡,¶}

Department of Mathematics

Michigan State University, MI 48824, USA, Department of Electrical and Computer Engineering

*Michigan State University, MI 48824, USA, and Department of Biochemistry and Molecular
Biology*

Michigan State University, MI 48824, USA

E-mail: wei@math.msu.edu

Abstract

Poisson-Boltzmann (PB) model is one of the most popular implicit solvent models in biophysical modeling and computation. The ability of providing accurate and reliable PB estimation of electrostatic solvation free energy, ΔG_{el} , and binding free energy, $\Delta\Delta G_{el}$, is important to computational biophysics and biochemistry. Recently, it has been warned in the literature (Journal of Chemical Theory and Computation 2013, 9, 3677-3685) that the widely used grid spacing of 0.5 Å produces unacceptable errors in $\Delta\Delta G_{el}$ estimation with the solvent exclude surface (SES). In this work, we investigate the grid dependence of our PB solver (MIBPB)

*To whom correspondence should be addressed

[†]Department of Mathematics

Michigan State University, MI 48824, USA

[‡]Department of Electrical and Computer Engineering

Michigan State University, MI 48824, USA

[¶]Department of Biochemistry and Molecular Biology

Michigan State University, MI 48824, USA

[§]The first two authors contribute equally to this work

with SESs for estimating both electrostatic solvation free energies and electrostatic binding free energies. It is found that the relative absolute error of ΔG_{el} obtained at the grid spacing of 1.0 Å compared to ΔG_{el} at 0.2 Å averaged over 153 molecules is less than 0.2%. Our results indicate that the use of grid spacing 0.6 Å ensures accuracy and reliability in $\Delta\Delta G_{\text{el}}$ calculation. In fact, the grid spacing of 1.1 Å appears to deliver adequate accuracy for high throughput screening.

1 Introduction

Electrostatics is ubiquitous in biomolecular and cellular systems and of paramount importance to biological processes. Accurate and reliable prediction of electrostatic binding free energy, $\Delta\Delta G_{\text{el}}$, is crucial to biophysical modeling and computation. The prediction of $\Delta\Delta G_{\text{el}}$ plays a vital role in the study of many cellular processes, such as signal transduction, gene expression, and protein synthesis. Additionally, many pharmaceutical applications, specially in the final stage of the drug design, rely on the accurate and reliable calculation of binding free energy. Technically, the accuracy and reliability of electrostatic binding energy prediction depend essentially on the quality of electrostatic solvation (ΔG_{el}) estimation, which can be achieved by solving the Poisson-Boltzmann (PB) equation in the implicit solvent model.¹⁻⁵ In past decades, the development of a robust PB solver catches much attention in computational biophysics and biochemistry. Mathematically, most PB solvers reported in the literature are based on three major approaches, namely, the finite difference method (FDM),⁶ the finite element method (FEM),⁷ and the boundary element method (BEM).^{8,9} Among them, the FDM is prevalently used in the field due to its simplicity in implementation. The emblematic solvers in this category are Amber PBSA,^{10,11} Delphi,^{12,13} APBS¹⁴ and CHARMM PBEQ.⁶

Recently, it has been warned that “the widely used grid spacing of 0.5 Å produces unacceptable errors in $\Delta\Delta G_{\text{el}}$ ”.¹⁵ Although all results were obtained with the adaptive Cartesian grid (ACG) finite difference PB equation solver¹⁶ in this work, similar results were reported in a later study¹⁷ by using APBS, DelPhi and PBSA. Therefore, these studies have arisen serious concerns about

the validity of using PB model for biomolecular electrostatic binding analysis at an affordable grid spacing of 0.5 Å.

In the past few years, there have been many attempts to develop highly accurate PB solvers using advance techniques for interface treatments.^{16,18–20} The later verison of the ACG solver^{16,18} has somewhat remedied the grid-dependence issue for estimates of binding energy. However, no confirmation for the reliable use of grid spacing of 0.5 Å in $\Delta\Delta G_{el}$ has been given. In this work, we investigate the grid dependence of our PB solver (MIBPB)^{21,22} in estimating both electrostatic solvation free energies and electrostatic binding free energies. The MIBPB solver is by far the only existing method that is second-order accurate in L_∞ norm for solving the Poisson-Boltzmann equation with discontinuous dielectric constants, singular charge sources, and geometric singularities from the solvent excluded surfaces (SEs) of biomolecules.²¹ Here the L_∞ norm means the maximum absolute error measure and “second order accurate” means that the error reduces four times when the grid spacing is halved. Contrary to the findings in the literature,¹⁵ our results indicate that the use of grid spacing 0.6 Å ensures accuracy and reliability in $\Delta\Delta G_{el}$ calculation. In fact, a grid spacing of 1.1 Å appears to deliver adequate accuracy for high throughput screening. We therefore believe that when it is used properly, the PB methodology is able to deliver accurate and reliable electrostatic binding analysis.

2 Methods

2.1 MIBPB package

In the current work, we employ the our MIBPB package^{21,22} to predict the electrostatic solvation free energy. The MIBPB package is a second-order convergence PB solver for dealing with the SEs of biomolecules. Numerically, there are three major obstacles in constructing accurate and reliable PB solvers. First, commonly used solvent-solute interfaces, i.e., the van der Waals (vdW) surface, solvent accessible surface (SAS), and the solvent excluded surface (SES)^{23,24} admit geometric singularities, such as sharp tips, cusps and self-intersecting surfaces,²⁵ which make the

rigorous enforcement of interface jump conditions a formidable task in PB solvers. An advanced mathematical interface techniques, the matched interface and boundary (MIB) method,^{26–31} is employed in the MIBPB package to achieve the second order accuracy in handling biomolecular SESs. Additionally, the atomic singular charges described by the delta functions give rise to another difficulty in constructing highly accurate PB solver. A Dirichlet-to-Neumann map technique has been developed in the MIBPB package to avoid the numerical approximation of singular charges by using the analytical Green’s functions.³² Finally, the nonlinear Boltzmann term can affect solver efficiency when handled inappropriately, particularly for BEMs. A quasi-Newton algorithm is implemented in the MIBPB package^{21,22} to take care the nonlinear term.^{21,22}

2.2 Interface generation

Many studies suggest that SES is able to deliver the state of the art accurate modeling of the solvated molecule.^{7,9,13} As a result, much effort has been paid to developing an accurate and robust SES software.^{25,33} However, the MSMS software²⁵ generates a Lagrangian representation of the SES and is inconvenient for the Cartesian domain implementation of PB solvers. A Lagrangian to Eulerian transformation is required to convert MSMS surfaces for our Cartesian based MIBPB solver.⁴ Most recently, we have developed a new SES software, Eulerian solvent excluded surface (ESES), to directly generate the SESs in the Eulerian representation.³⁴ Our ESES software enables the MIBPB solver to produce a reliable ΔG_{el} . Both MSMS and ESES are supported by our MIBPB software. By increasing the MSMS surface density, the electrostatic solvation free energies calculated by using MSMS converge to those obtained by using ESES.³⁴ Therefore, only results employing ESES are shown in this work.

2.3 Data sets

In the present work, we adopt three sets of biomolecular complexes employed in the literature¹⁵ for solvation free energy and binding free energy estimations. Specifically, the first set, Data Set 1, is a collection of DNA-minor groove drug complexes having a narrow range of $\Delta\Delta G$.

The Protein Data Bank (PDB) IDs (PDBIDs) for this set are as follows: 102d, 109d, 121d, 127d, 129d, 166d, 195d, 1d30, 1d63, 1d64, 1d86, 1dne, 1eel, 1fmq, 1fms, 1jtl, 1lex, 1prp, 227d, 261d, 164d, 289d, 298d, 2dbe, 302d, 311d, 328d, and 360d. The second set, Data Set 2, includes various wild-type and mutant barnase-barstar complexes. Its PDBIDs are as follows: 1b27, 1b2s, 1b2u, 1b3s, 2aza4, 1x1w, 1x1y, 1x1u, and 1x1x. In the last set, Data Set 3, we investigate RNA-peptide complexes with following PDBIDs: 1a1t, 1a4t, 1biv, 1exy, 1g70, 1hji, 1i9f, 1mnb, 1nyb, 1qfq, 1ull, 1zbn, 2a9x, and 484d. The detail of the structural preprocessing can be found in Ref. Harris et al.. The data sets can be downloaded from website http://www.sb.fsu.edu/~mfenley/convergence/downloads/convergence_pqr_sets.tar.gz. They are also available from the present authors upon request.

2.4 Poisson-Boltzmann calculation details

The electrostatics binding free energy is a measure of binding affinity of two compounds due to the electrostatics interaction. Based on the free energy cycle, the electrostatics binding free energy can be calculated by the following formula³⁵

$$\Delta\Delta G_{\text{el}} = (\Delta G_{\text{el}})_{\text{AB}} - (\Delta G_{\text{el}})_{\text{A}} - (\Delta G_{\text{el}})_{\text{B}} + (\Delta\Delta G_{\text{el}})_{\text{Coulomb}}, \quad (1)$$

where $(\Delta G_{\text{el}})_{\text{AB}}$ is the electrostatic solvation free energy of the bounded complex AB, $(\Delta G_{\text{el}})_{\text{A}}$ and $(\Delta G_{\text{el}})_{\text{B}}$ are the electrostatic solvation free energies of the unbounded components A and B, and $(\Delta\Delta G_{\text{el}})_{\text{Coulomb}}$ is the electrostatic binding free energy of the two components in vacuum.

The electrostatic solvation free energies ΔG_{el} are obtained by using MIBPB software^{21,22} while the binding energy $(\Delta\Delta G_{\text{el}})_{\text{Coulomb}}$ is easily evaluated analytically via the following formula

$$(\Delta\Delta G_{\text{el}})_{\text{Coulomb}} = \sum_{i,j} \frac{q_i q_j}{\epsilon_m r_{ij}}, \quad \forall i \in \text{A}, j \in \text{B}, \quad (2)$$

where q_i and q_j are the corresponding charges of the given pair of atoms, and r_{ij} is the distance between this pair. Here, ϵ_m is the dielectric constant of the solute region. Table S3 (in the supporting

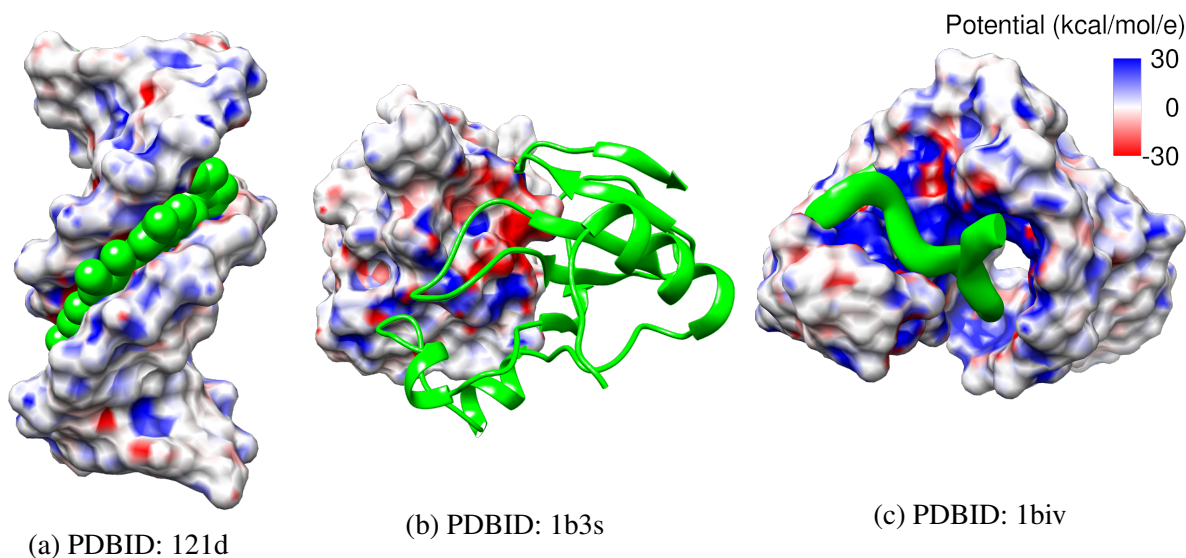


Figure 1: Illustration of surface electrostatic potentials (in units of kcal/mol/e) for three complexes, generated by Chimera software.³⁶ (a) PDBID: 121d (in Drug-DNA complexes); (b) PDBID: 1b3s (in barnase-barstar complexes); (c) PDBID: 1biv (in RNA-peptide complexes).

information) lists $(\Delta\Delta G_{el})_{\text{Coulomb}}$ values of 51 studied complexes.

In all our calculations, the absolute temperature of the ionic solvent is chosen to be $T = 298$ K, the dielectric constants for solute and solvent are 1 and 80, and the ionic strength is 0.1 M NaCl. The PBE is solved by the linearized solver, but the nonlinear one does not produce any notably differences. The incomplete LU biconjugate gradient squared (ILUBGS) solver is employed to solve all linear systems risen by the MIBPB approach. To maintain consistent computations of the PB solver at different grid sizes, the criteria convergence of ILUBGS solver measured by L_2 -norm is set to be 10^{-6} , and the maximum iteration number is set to 100,000. The predictions of MIBPB solver on ΔG_{el} and $\Delta\Delta G_{el}$ are confirmed by other solvers such as PBSA,^{10,11} Delphi,^{12,13} and APBS¹⁴ at the grid size of 0.2 Å, see Table S2 of Supporting Information.

3 Results and discussion

As described above, we consider three sets of binding complexes, namely, drug-DNA, barnase-barstar and RNA-peptide systems. For the sake of illustration, three sample surface electrostatic potentials, each from one distinct set, are depicted in Fig. 1. PDBIDs for these three complexes

Table 1: R^2 values and best fitting lines of electrostatic solvation free energies with different grid sizes.

	Grid sizes (pair)	R^2	Best fitting line
DNA-drug	(0.2,0.3)	1.0000	$y = 1.0000x - 0.0196$
	(0.2,0.4)	1.0000	$y = 1.0000x - 0.0081$
	(0.2,0.5)	1.0000	$y = 1.0001x - 0.0621$
	(0.2,0.6)	1.0000	$y = 1.0001x - 0.2230$
	(0.2,0.7)	1.0000	$y = 1.0003x - 0.2537$
	(0.2,0.8)	1.0000	$y = 1.0003x - 0.4161$
	(0.2,0.9)	1.0000	$y = 1.0003x - 0.2999$
	(0.2,1.0)	1.0000	$y = 1.0005x - 0.0066$
	(0.2,1.1)	1.0000	$y = 1.0004x - 0.2485$
Barnase-barstar	(0.2,0.3)	1.0000	$y = 1.0002x + 0.1590$
	(0.2,0.4)	1.0000	$y = 1.0005x + 0.3524$
	(0.2,0.5)	1.0000	$y = 1.0012x + 0.8735$
	(0.2,0.6)	1.0000	$y = 1.0010x - 0.2246$
	(0.2,0.7)	1.0000	$y = 1.0017x - 0.3748$
	(0.2,0.8)	1.0000	$y = 1.0009x - 0.9576$
	(0.2,0.9)	0.9999	$y = 1.0015x + 0.4749$
	(0.2,1.0)	0.9999	$y = 0.9986x - 2.9739$
	(0.2,1.1)	0.9997	$y = 0.9972x - 4.3801$
RNA-peptide	(0.2,0.3)	1.0000	$y = 1.0000x - 0.0445$
	(0.2,0.4)	1.0000	$y = 1.0000x - 0.1333$
	(0.2,0.5)	1.0000	$y = 1.0000x - 0.3343$
	(0.2,0.6)	1.0000	$y = 1.0000x - 0.1916$
	(0.2,0.7)	1.0000	$y = 1.0001x - 0.5377$
	(0.2,0.8)	1.0000	$y = 1.0001x - 0.8198$
	(0.2,0.9)	1.0000	$y = 1.0002x - 0.9564$
	(0.2,1.0)	1.0000	$y = 1.0003x - 0.8868$
	(0.2,1.1)	1.0000	$y = 1.0005x - 2.2504$

are respectively 121d (in Drug-DNA complexes), 1b3s (in barnase-barstar complexes), and 1biv (in RNA-peptide complexes). In the rest of this section, we explore the influence of grid spacing in Poisson-Boltzmann equation solvation and binding free energy estimations using our MIBPB solver.

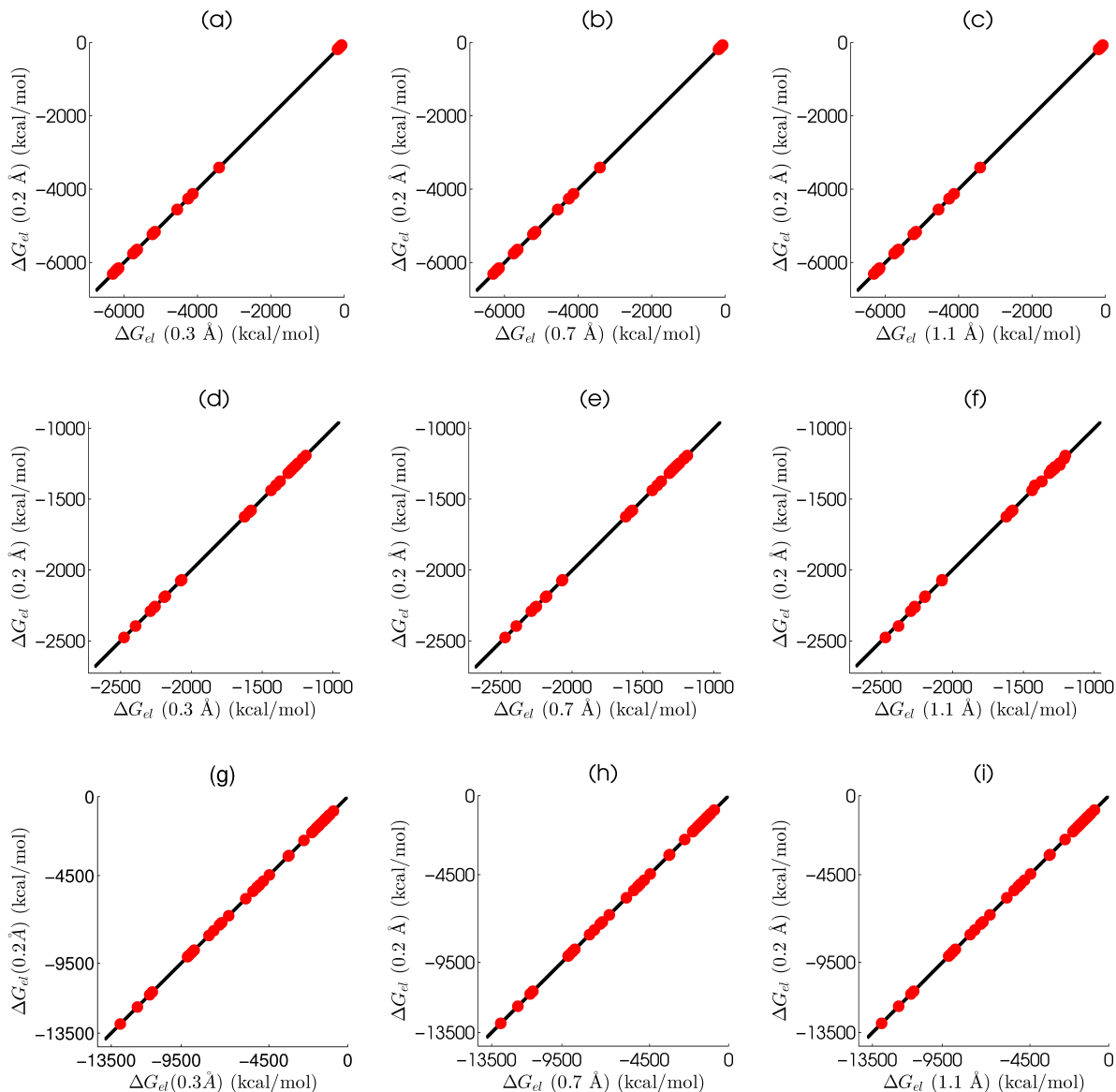


Figure 2: Electrostatic solvation free energy, for all complexes and unbounded components of three data sets, with different grid sizes plotted against the one computed with a finest grid size of $h = 0.2 \text{ \AA}$. (a) DNA-drug with pair $(0.2 \text{ \AA}, 0.3 \text{ \AA})$; (b) DNA-drug with pair $(0.2 \text{ \AA}, 0.7 \text{ \AA})$; (c) DNA-drug with pair $(0.2 \text{ \AA}, 1.1 \text{ \AA})$; (d) Barnase-barstar with pair $(0.2 \text{ \AA}, 0.3 \text{ \AA})$; (e) Barnase-barstar with pair $(0.2 \text{ \AA}, 0.7 \text{ \AA})$; (f) Barnase-Barstar with pair $(0.2 \text{ \AA}, 1.1 \text{ \AA})$; (g) RNA-peptide with pair $(0.2 \text{ \AA}, 0.3 \text{ \AA})$; (h) RNA-peptide with pair $(0.2 \text{ \AA}, 0.7 \text{ \AA})$; (i) RNA-peptide with pair $(0.2 \text{ \AA}, 1.1 \text{ \AA})$.

3.1 The influence of grid spacing in ΔG_{el} estimation

We first examine the accuracy and robustness of our MIBPB solver in predicting the electrostatic solvation free energies of the aforementioned three data sets. Some previous literature^{37,38} has

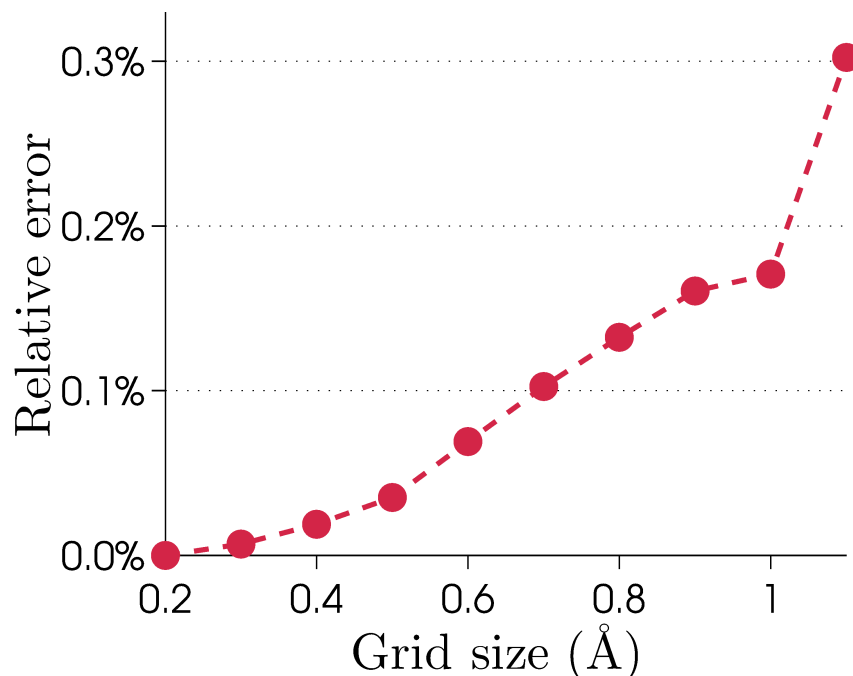


Figure 3: Averaged relative absolute error of the electrostatic solvation free energies for all the 153 molecules with mesh size refinements from 1.1 Å to 0.2 Å.

recognized that a grid size of $h = 0.5 \text{ \AA}$ is small enough to produce a reliable ΔG_{el} . Such an observation certainly remains for the MIBPB solver. In fact, our PB solver is able to deliver a very well-convergent calculations of electrostatic solvation free energies at as coarse grid sizes as 1.0 Å and 1.1 Å.

In the current calculations, the finest grid size is chosen to be 0.2 Å, and the coarser grid sizes are between 0.3 Å and 1.1 Å. Figure 2 depicts the correlations of ΔG_{el} at various meshes for all complexes and unbounded components of three data sets. The electrostatic solvation free energies obtained at the finest grid spacing of 0.2 Å are plotted against those computed from coarser grid spacings of 0.3 Å, 0.7 Å and 1.1 Å. Obviously, the best fitting lines for these data at various coarse grid spacings produce near perfect alignments between the finest mesh results and those from coarse meshes. As shown in Table 1, R^2 and slope values at the pair of grid sizes (0.2 Å, 1.1 Å) for DNA-drug, barnase-barstar and RNA-peptide are, respectively, (1.0000, 1.0004), (0.9997, 0.9972), and (1.0000, 1.0005). These results indicate the accuracy and robustness in the

MIBPB prediction of electrostatic solvation free energies (ΔG_{el}). Table S1, in the Supporting Information, reports the values ΔG_{el} for all the 51 complexes and associated 102 components studied in this work. Finally, we examine the performance of our solver by considering the relative absolute error, the difference between results obtained with coarser and the finest grid spacings, defined as follows

$$\text{Relative absolute error} \doteq \left| \frac{\Delta G_{\text{el},h} - \Delta G_{\text{el},h=0.2}}{\Delta G_{\text{el},h=0.2}} \right|. \quad (3)$$

Figure 3 illustrates the averaged relative absolute errors, i.e., the average of relative absolute errors designated in Eq. (3) over all the 153 discussed molecules, at different mesh sizes. It can be seen from Fig. 3 that the averaged relative absolute errors at all studied cases are less than 0.31%, and for any grid spacing smaller than 1.1 Å, these errors are always below 0.2%. This behavior further indicates the grid size independence of our PB solver over the normal grid-size range in molecular biophysical applications.

3.2 The influence of grid spacing in $\Delta\Delta G_{\text{el}}$ estimation

Motivated by well-converged estimations of electrostatic solvation free energies at very coarse grid spacings as previously discussed, we are interested in predicting the binding free energies for all RNA-drug, barnase-barstar, and RNA-peptide complexes using our MIBPB package.

Similar to the study of the convergence of ΔG_{el} , we correlate the binding free energy calculated at the finest grid spacing, $h = 0.2 \text{ \AA}$, and ones estimated at coarser mesh sizes, $h = 0.3 \text{ \AA}, \dots, 1.1 \text{ \AA}$. Figure 4 illustrates these relationships with the regression lines whose parameters are revealed in Table 2. Since the previous discussion confirms MIBPB solver can produce very good R-squared values even at very coarse grid spacings, it is interesting to explore whether a similar behavior can be found for binding energy estimation. Indeed, the PB binding energy estimation behaves the same as the PB solvation calculation in our MIBPB technique. Specifically, R^2 is always 1 at the fine mesh, $h = 0.3 \text{ \AA}$. Moreover, these values are still satisfactory at relatively coarser mesh sizes. For example, at the grid spacing of $h = 1.1$, the R^2 and slope of the regression line for DNA-drug,

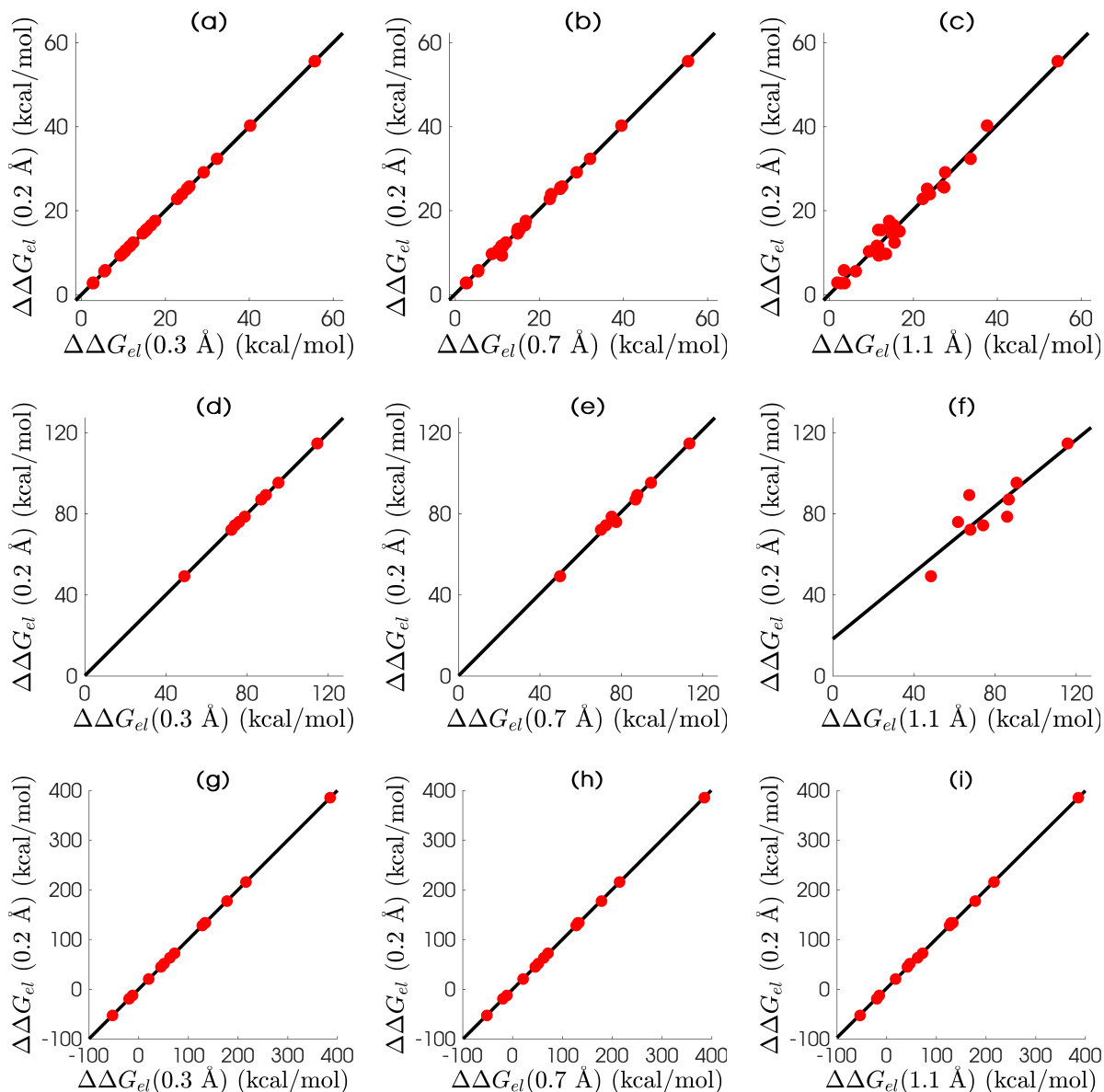


Figure 4: Electrostatic binding free energy, for all complexes with different grid sizes plotted against the one computed with a finest grid size of $h = 0.2 \text{ \AA}$. (a) DNA-drug with pair $(0.2 \text{ \AA}, 0.3 \text{ \AA})$; (b) DNA-drug with pair $(0.2 \text{ \AA}, 0.7 \text{ \AA})$; (c) DNA-drug with pair $(0.2 \text{ \AA}, 1.1 \text{ \AA})$; (d) Barnase-barstar with pair $(0.2 \text{ \AA}, 0.3 \text{ \AA})$; (e) Barnase-barstar with pair $(0.2 \text{ \AA}, 0.7 \text{ \AA})$; (f) Barnase-barstar with pair $(0.2 \text{ \AA}, 1.1 \text{ \AA})$; (g) RNA-peptide with pair $(0.2 \text{ \AA}, 0.3 \text{ \AA})$; (h) RNA-peptide with pair $(0.2 \text{ \AA}, 0.7 \text{ \AA})$; (i) RNA-peptide with pair $(0.2 \text{ \AA}, 1.1 \text{ \AA})$.

barnase-barstar, and RNA-peptide complexes are, respectively, $(0.9747, 1.0081)$, $(0.8002, 0.8187)$, and $(0.9998, 0.9937)$. In contrast, the R-squared values reported in Ref.¹⁵ computed between 0.3 \AA and 1.0 \AA , are unacceptable for SESs, and usually less than 0.62. Our statistical measures

Table 2: R^2 values and best fitting lines of electrostatic binding free energies with different grid sizes.

	Grid sizes (pair)	R^2	Best fitting line
DNA-drug	(0.2,0.3)	1.0000	$y = 0.9993x + 0.0194$
	(0.2,0.4)	0.9999	$y = 0.9987x + 0.0273$
	(0.2,0.5)	0.9998	$y = 1.0028x + 0.0164$
	(0.2,0.6)	0.9991	$y = 1.0047x + 0.2256$
	(0.2,0.7)	0.9982	$y = 1.0074x + 0.1394$
	(0.2,0.8)	0.9966	$y = 1.0110x + 0.1484$
	(0.2,0.9)	0.9906	$y = 0.9655x + 1.2385$
	(0.2,1.0)	0.9875	$y = 0.9827x + 0.5894$
	(0.2,1.1)	0.9747	$y = 1.0081x + 0.0709$
Barnase-barstar	(0.2,0.3)	0.9999	$y = 0.9974x + 0.2035$
	(0.2,0.4)	0.9995	$y = 0.9997x - 0.0492$
	(0.2,0.5)	0.9923	$y = 1.0318x - 2.7755$
	(0.2,0.6)	0.9946	$y = 0.9878x + 1.5525$
	(0.2,0.7)	0.9932	$y = 1.0090x + 0.1819$
	(0.2,0.8)	0.9883	$y = 0.9766x + 3.7333$
	(0.2,0.9)	0.9493	$y = 0.9382x + 5.3970$
	(0.2,1.0)	0.9384	$y = 1.0912x - 3.8377$
	(0.2,1.1)	0.8002	$y = 0.8187x + 18.2837$
RNA-peptide	(0.2,0.3)	1.0000	$y = 0.9997x - 0.0655$
	(0.2,0.4)	1.0000	$y = 1.0001x - 0.1106$
	(0.2,0.5)	1.0000	$y = 1.0012x - 0.2755$
	(0.2,0.6)	1.0000	$y = 0.9999x + 0.2021$
	(0.2,0.7)	0.9999	$y = 1.0037x - 0.3756$
	(0.2,0.8)	1.0000	$y = 1.0004x + 0.6673$
	(0.2,0.9)	0.9999	$y = 0.9927x + 1.9755$
	(0.2,1.0)	0.9997	$y = 0.9923x + 2.8775$
	(0.2,1.1)	0.9998	$y = 0.9937x + 1.7992$

strongly support the reliable binding energy prediction of our solver at coarse grid sizes. Table 3 displays the binding free energy for all complexes with different grid spacings. As can be seen from Table 3, the difference between binding energies at coarse meshes and the finest mesh, $h = 0.2 \text{ \AA}$, is mostly less than 10 kcal/mol for all complexes.

The trend of binding free energy at different grid spacings can be seen clearly in Figs. 5 which plots $\Delta\Delta G_{el}$ against grid sizes varying between 0.2 \AA and 1.1 \AA for DNA-drug complexes. Similar

Table 3: Electrostatic binding free energies (in units of kcal/mol), $\Delta\Delta G_{el}$, for all of the complexes used in this study at different grid sizes.

	complexes	1.1 Å	1.0 Å	0.9 Å	0.8 Å	0.7 Å	0.6 Å	0.5 Å	0.4 Å	0.3 Å	0.2 Å	
DNA-drug	102d	9.45	10.50	8.73	10.01	10.21	10.76	10.53	10.45	10.34	10.31	
	109d	3.61	2.18	2.30	3.72	2.63	2.07	2.66	2.69	2.82	2.72	
	121d	23.95	23.99	23.80	24.05	22.84	23.65	24.10	23.94	23.96	23.93	
	127d	27.60	28.80	28.45	28.89	28.88	28.93	29.27	29.16	29.12	29.12	
	129d	37.58	40.23	39.92	39.03	39.52	39.90	40.04	40.15	40.20	40.24	
	166d	15.04	16.60	13.97	14.93	14.91	15.49	15.47	15.62	15.67	15.67	
	195d	2.74	3.73	2.80	2.63	2.77	2.77	2.63	2.69	2.72	2.73	
	1d30	11.27	10.01	10.71	9.31	10.26	10.12	10.40	10.75	10.53	10.59	
	1d63	15.51	12.83	7.08	12.56	12.07	11.24	12.10	12.29	12.34	12.39	
	1d64	14.98	14.11	14.26	14.03	14.86	14.24	14.51	14.57	14.59	14.58	
	1d86	27.37	25.53	24.50	25.88	25.04	25.57	25.39	25.44	25.50	25.54	
	1dne	22.26	22.73	22.32	22.92	22.48	22.62	22.58	22.74	22.83	22.81	
	1eel	16.71	17.06	14.94	14.82	14.77	14.60	15.08	14.85	15.15	15.07	
	1fmq	12.35	13.40	14.28	14.72	15.27	15.09	15.30	15.36	15.36	15.37	
	1fms	27.08	26.14	25.17	24.52	25.41	25.93	25.82	25.75	25.71	25.74	
	1jtl	11.62	10.99	11.80	11.47	11.30	11.28	11.37	11.28	11.41	11.45	
	1lex	13.47	10.37	9.79	9.44	8.74	9.74	9.81	9.70	9.70	9.70	
	1prp	11.30	11.93	10.78	10.88	11.01	11.55	11.55	11.49	11.61	11.61	
	227d	6.28	4.79	5.96	3.79	5.47	5.16	5.80	5.75	5.46	5.58	
	261d	1.91	3.00	1.75	1.55	2.60	2.79	2.97	2.76	2.80	2.85	
	264d	33.64	32.35	31.57	30.83	32.09	31.97	32.07	32.20	32.31	32.34	
	289d	15.32	15.71	17.94	16.70	16.57	16.21	16.22	16.56	16.59	16.56	
	298d	11.65	15.94	14.81	15.89	14.87	14.88	15.38	15.45	15.50	15.41	
	2dbe	3.48	5.06	3.49	6.14	5.51	5.77	5.76	5.88	5.68	5.81	
	302d	23.28	25.22	24.91	25.49	24.95	25.00	24.87	25.29	25.17	25.19	
	311d	11.76	3.36	7.15	9.72	11.12	8.17	8.98	9.34	9.30	9.32	
	328d	14.25	16.21	17.38	17.85	16.79	17.14	17.84	17.68	17.54	17.54	
	360d	54.41	54.72	56.63	54.59	55.38	54.56	55.44	55.80	55.61	55.57	
	Barnase-barstar	1b27	86.80	83.08	95.40	82.48	87.05	89.40	87.35	87.96	86.96	87.05
		1b2s	67.80	66.33	68.81	71.75	70.03	71.47	72.32	71.93	72.25	72.12
		1b2u	85.97	76.39	74.78	78.29	75.29	77.35	77.15	78.38	78.87	78.57
		1b3s	48.41	56.58	49.61	46.02	49.87	48.17	53.44	49.38	49.07	49.25
		1x1u	61.75	66.86	74.53	75.07	77.56	76.56	75.06	76.41	76.06	75.95
		1x1w	90.62	87.91	99.13	93.67	94.65	93.55	95.53	95.32	95.47	95.30
		1x1x	115.79	110.40	110.45	112.19	113.51	114.45	115.30	114.65	114.62	114.65
		1x1y	67.27	88.13	89.80	90.39	87.87	87.24	88.54	88.91	89.20	89.21
2za4		74.13	70.86	70.64	69.80	72.45	73.22	73.26	74.18	74.00	74.35	
RNA-peptide		1a1t*	62.24	58.24	61.71	61.89	62.94	63.18	62.88	62.75	62.95	63.00
		1a4t*	72.37	72.44	69.76	69.94	71.19	72.46	72.41	72.39	72.24	72.27
		1biv*	41.80	40.73	42.07	44.90	45.66	44.70	44.69	44.75	44.86	44.76
	1exy*	178.36	178.17	178.16	176.29	178.70	176.91	177.52	177.50	177.70	177.36	
	1g70	133.22	131.38	132.83	132.75	132.83	133.85	133.94	134.37	134.34	133.53	
	1hji	46.78	46.06	49.80	50.70	51.51	51.26	51.21	51.42	51.17	51.23	
	1i9f	-19.78	-22.55	-22.49	-19.44	-19.31	-19.20	-19.18	-19.18	-19.20	-19.22	
	1mnb	126.65	129.00	127.74	126.95	127.80	127.82	128.30	128.15	128.15	128.20	
	1nyb	-14.63	-13.07	-13.62	-12.58	-11.16	-13.04	-12.79	-12.45	-12.41	-12.61	
	1qfq	18.09	19.84	16.64	20.52	21.19	20.03	22.60	20.66	20.19	20.32	
	1ull*	-53.38	-58.11	-54.20	-53.61	-51.66	-53.28	-52.52	-52.76	-52.66	-52.75	
	1zbn*	216.31	214.29	215.60	214.96	214.84	216.05	215.70	215.95	215.94	215.74	
2a9x	385.99	384.41	385.18	385.36	385.05	385.20	385.36	385.36	385.43	385.44		
484d*	129.72	129.65	133.42	132.09	131.34	132.03	132.79	133.20	133.23	133.38		

* Results are significantly different (>50 kcal/mol) from those in Ref. ¹⁵

figures for barnase-barstar and RNA-peptide complexes can be referred to Figs. S1 and S2 in the Supporting Information. Based on these figures, our solver can rank the binding free energy for DNA-drug complexes at grid spacing of 0.6 Å, barnase-barstar complexes at grid spacing of 0.6 Å,

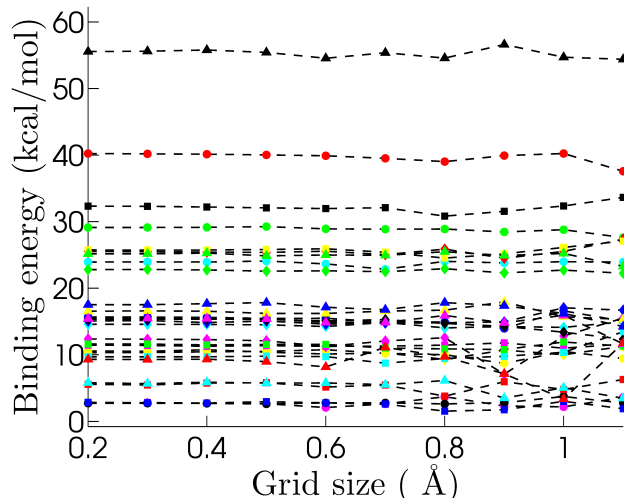


Figure 5: Binding electrostatic energy for DNA-drug complexes with grid sizes from 0.2 Å to 1.1 Å. The markers and PDBIDs are as follows yellow circle : 102d, magenta circle : 109d, cyan circle : 121d, green circle : 127d, red circle : 129d, blue circle : 166d, black circle : 195d, yellow diamond : 1d30, magenta diamond : 1d63, cyan diamond : 1d64, green diamond : 1d86, red diamond : 1dne, blue diamond : 1eel, black diamond : 1fmq, yellow square : 1fms, magenta square : 1jtl, cyan square : 1lex, green square : 1prp, red square : 227d, blue square : 261d, black square : 264d, yellow triangle: 289d, magenta triangle: 298d, cyan triangle: 2dbe, green triangle: 302d, red triangle: 311d, blue triangle: 328d, black triangle: 360d.

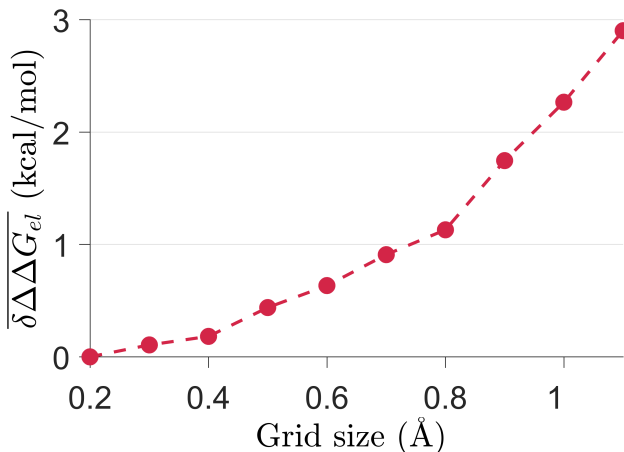


Figure 6: Averaged absolute error of the binding free energies for all the 51 complexes with mesh size refinements from 1.1 Å to 0.2 Å.

and RNA-peptide complexes at significantly coarse grid spacing of 1.1 Å. To further assess the reliable estimates of binding energy of our MIBPB solver, we consider the absolute difference

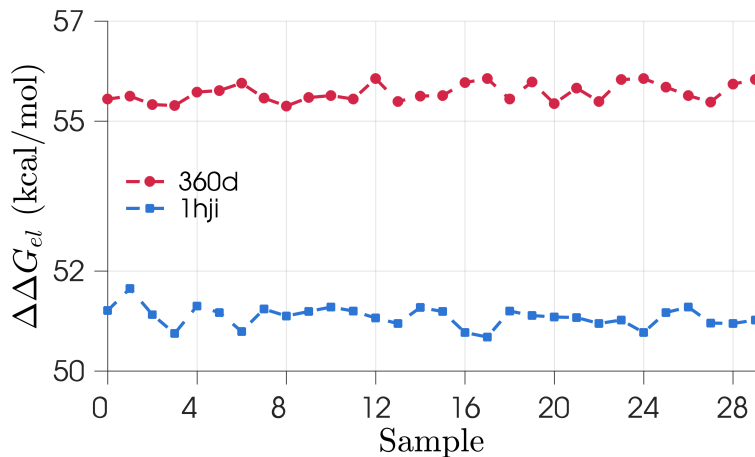


Figure 7: Binding energies of two complexes PDB IDs: 360d (marked by circle) and 1hji (marked by square) at 30 different grid positions.

between results computed at a coarser grid spacing and the finest grid spacing defined by

$$\delta\Delta\Delta G_{el} = |\Delta\Delta G_{el,h} - \Delta\Delta G_{el,h=0.2}|. \quad (4)$$

Figure 6 plots the averaged absolute errors, $\overline{\delta\Delta\Delta G_{el}}$, i.e., the average of absolute errors defined in Eq. (??) over all 51 complexes, at different mesh sizes. It is seen that even the use of grid spacing of 0.7 \AA still delivers an averaged binding calculation error under 1 kcal/mol for this set of complexes. Therefore, we can draw a conclusion that the common use of grid size being 0.5 \AA is still adequate for predicting the binding energy free without producing a misleading result.

Grid positioning error is another feature to validate the robustness and accuracy of a PB solver. To examine such numerical error for our MIBPB solver, we consider two protein complexes with PDBIDs: 360d and 1hji. To estimate the standard deviation, σ_{bd} in $\Delta\Delta G_{el}$, we randomly generate 29 grid positions around the initial origin with the amplitude of the random seed being $\pm 0.5h$, where $h = 0.5 \text{ \AA}$ is the grid spacing. Then $\Delta\Delta G_{el}$ is evaluated at all of the 30 grid positions. Figure 7 plots electrostatic binding energies at 30 distinct samples of grid positions, including the original one marked by Sample 0 on the graph. The σ_{bd} values of complexes 360d and 1hji are found to be 0.18 and 0.21, respectively. These results indicate that the MIBPB solver is not

sensitive to grid position.

Note that in Table 3, some binding energies obtained in our calculations, all from RNA-peptide complexes, differ significantly from those reported in Ref.,¹⁵ i.e., more than 50 kcal/mol at the finest grid spacing, under the same parametrization and data inputs. However, overall, our results have a good agreement with those in Ref.¹⁵ with $R^2 = 0.9135$ for RNA-peptide complexes. To further support our calculations, we have employed PBSA, Delphi, and APBS for electrostatic energy calculations at the grid size of 0.2 Å. We note that results obtained from these solvers are in excellent agreements, i.e., $R^2 > 0.98$, with ours. The electrostatic energies calculated by PBSA, Delphi, and APBS solvers are listed in Table S2 of Supporting Information.

4 Concluding remarks

Poisson-Boltzmann (PB) theory is an established model for biomolecular electrostatic analysis and has been widely used in electrostatic solvation ΔG_{el} and binding energy $\Delta\Delta G_{\text{el}}$ estimations. However, doubt has been cast on the validity of the commonly used grid spacing of 0.5 Å for producing converged estimates of $\Delta\Delta G_{\text{el}}$ due to the unacceptable errors observed in the calculation using the solvent excluded surface (SES) and the adaptive Cartesian grid (ACG) finite difference PB equation solver.¹⁵ Three sets of biomolecular complexes, namely, DNA-drug complexes, barnase-barstar complexes, and RNA-peptide complexes, are employed in the study. The discrepancies between results obtained from different surface definitions were also utilized to support the general pessimism for the PB methodology.

In this work, we employ the MIBPB software^{21,32} to estimate electrostatic solvation free energy, ΔG_{el} , and binding free electrostatic energy, $\Delta\Delta G_{\text{el}}$, for the three sets of biomolecular complexes used in Ref.¹⁵ The popular SES is adopted in the present work. In our ΔG_{el} estimation, the averaged relative absolute error computed at a relatively coarse grid size of 1.1 Å against the finest grid size of 0.2 Å over 153 studied biomolecules is less than 0.31%. The same error obtained at the grid size of 1.0 Å is less than 0.2%. These results indicate the reliability of using the MIBPB

solver at the grid spacing of 1.0 Å or even 1.1 Å for electrostatic solvation analysis. The robustness and accuracy of MIBPB solver for estimates of ΔG_{el} have been reported for 24 proteins in the literature.^{21,32} This characteristics has been confirmed again in the present work for DNA-drug complexes, barnase-barstar complexes, and RNA-peptide complexes.

The well-converged ΔG_{el} produced by our solver enables a promising performance in predicting $\Delta\Delta G_{\text{el}}$ at a coarse grid spacing. Indeed, numerical estimates of $\Delta\Delta G_{\text{el}}$ in the current work reveals that $\Delta\Delta G_{\text{el}}$ obtained at a 1.1 Å grid spacing mostly differ by less than 10 kcal/mol from that achieved by using a 0.2 Å grid spacing. Moreover, MIBPB solver conducted at grid size of 0.6 Å perfectly produces a well-converged $\Delta\Delta G_{\text{el}}$, and qualitatively ranks the complexes in term of their binding free energies. Therefore, the current results support an opinion that the widely used grid size of 0.5 Å can give reliable and accurate enough predictions of both electrostatic free energy^{39,40} and binding free energy.

To develop highly accurate, robust and reliable PB solvers for biomolecular electrostatics, it is crucial to validate one's numerical methods by appropriate norms and against realistic problems. We emphasize that as an elliptic interface problem, it is important to measure the convergence of PB solvers in the L_{∞} norm, or maximum absolute error, because integral norms, such as L_1 and L_2 , are insensitive to the performance of numerical methods near the interface. Additionally, the convergence should be tested by solving the PB equation, rather than by calculating the solvation free energy. Finally, validation should be carried out by using the SESs of proteins, rather than smooth surfaces, such as a sphere.

Supporting Information Available

Electrostatic free energies calculated by different solvers, namely MIBPB, DELPHI, PBSA and APBS; Coulombic binding energies; binding energy plots for barnase-barstar and RNA-peptide complexes (filename: jctc_si_bdenergy.pdf).

This material is available free of charge via the Internet at <http://pubs.acs.org/>.

Acknowledgement

This work was supported in part by NSF Grant Nos. IIS- 1302285 and DMS-1160352, NIH Grant No. R01GM-090208 and MSU Center for Mathematical Molecular Biosciences Initiative. DDN and GWW thank the Mathematical Biosciences Institute for its hospitality and support during their visit in Ohio State University, where this manuscript was finalized. This manuscript was reviewed by Professors Emil Alexov and Ray Luo prior its submission.

References

- (1) Gilson, M. K.; Sharp, K.; Honig, B. Calculating the Electrostatic Potential of Molecules in Solution: Method and error assessment. *J. Comp. Chem.* **1987**, *9*, 327–335.
- (2) Gilson, M. K.; Davis, M. E.; Luty, B. A.; McCammon, J. A. Computation of electrostatic forces on solvated molecules using the Poisson-Boltzmann equation. *Journal of Physical Chemistry* **1993**, *97*, 3591–3600.
- (3) Talley, K.; Ng, C.; Shoppell, M.; Kundrotas, P.; Alexov, E. On the electrostatic component of protein-protein binding free energy. *PMC Biophysics* **2008**, *1:2*, 1–23.
- (4) Zhou, Y. C.; Feig, M.; Wei, G. W. Highly accurate biomolecular electrostatics in continuum dielectric environments. *Journal of Computational Chemistry* **2008**, *29*, 87–97.
- (5) Ren, P.; Chun, J.; Thomas, D. G.; Schnieders, M. J.; Marucho, M.; Zhang, J.; Baker, N. A. Biomolecular electrostatics and solvation: a computational perspective. *Quarterly reviews of biophysics* **2012**, *45(04)*, 427–491.
- (6) Jo, S.; Vargyas, M.; Vasko-Szedlar, J.; Roux, B.; Im, W. PBEQ-Solver for online visualization of electrostatic potential of biomolecules. *Nucleic Acids Research* **2008**, *36*, W270 –W275.
- (7) Baker, N. A.; Sept, D.; Holst, M. J.; Mccammon, J. A. The adaptive multilevel finite element solution of the Poisson-Boltzmann equation on massively parallel computers. *IBM Journal of Research and Development* **2001**, *45*, 427–438.

- (8) Geng, W. H.; Krasny, R. A treecode-accelerated boundary integral Poisson-Boltzmann solver for continuum electrostatics of solvated biomolecules. *J. Comput. Phys.* **2013**, *247*, 62–87.
- (9) Lu, B.; Cheng, X.; Huang, J.; McCammon, J. A. AFMPB: An Adaptive Fast Multipole Poisson-Boltzmann Solver for Calculating Electrostatics in Biomolecular Systems. *Comput. Phys. Commun.* **2013**, *184*, 2618–2619.
- (10) Wang, J.; Tan, C. H.; Tan, Y. H.; Lu, Q.; Luo, R. Poisson-Boltzmann solvents in molecular dynamics Simulations. *Communications in Computational Physics* **2008**, *3(5)*, 1010–1031.
- (11) Cai, Q.; Hsieh, M. J.; Wang, J.; Luo, R. Performance of Nonlinear Finite-Difference Poisson-Boltzmann Solvers. *Journal of Chemical Theory and Computation* **2009**, *6(1)*, 203–211.
- (12) Li, L.; Li, C.; Sarkar, S.; Zhang, J.; Witham, S.; Zhang, Z.; Wang, L.; Smith, N.; Petukh, M.; Alexov, E. Delphi: a comprehensive suite for Delphi software and associated resources. *BMC Biophysics* **2012**, *5:9*, 2046–1682.
- (13) Rocchia, W.; Sridharan, S.; Nicholls, A.; Alexov, E.; Chiabrera, A.; Honig, B. Rapid grid-based construction of the molecular surface and the use of induced surface charge to calculate reaction field energies: Applications to the molecular systems and geometric objects. *Journal of Computational Chemistry* **2002**, *23*, 128 – 137.
- (14) Baker, N. A.; Sept, D.; Joseph, S.; Holst, M. J.; McCammon, J. A. Electrostatics of nanosystems: Application to microtubules and the ribosome. *Proceedings of the National Academy of Sciences of the United States of America* **2001**, *98*, 10037–10041.
- (15) Harris, R. C.; Boschitsch, A. H.; Fenley, M. O. Influence of Grid Spacing in Poisson-Boltzmann Equation Binding Energy Estimation. *Journal of Chemical Theory and Computation* **2013**, *9*, 3677–3685.
- (16) Boschitsch, A. H.; Fenley, M. O. Chapter 4, The Adaptive Cartesian Grid-Based Poisson–Boltzmann Solver: Energy and Surface Electrostatic Properties, in *Computational Electro-*

- statics for Biological Applications: Geometric and Numerical Approaches to the Description of Electrostatic Interaction Between Macromolecules, Rocchia, W., Spagnuolo, M., Eds. *Cham, 2015* **2015**, 73–110.
- (17) Sorensen, J.; Fenley, M. O.; Amaro, R. E. Chapter 3, A Comprehensive Exploration of Physical and Numerical Parameters in the Poisson-Boltzmann Equation for Applications to Receptor-Ligand Binding, in *Computational Electrostatics for Biological Applications: Geometric and Numerical Approaches to the Description of Electrostatic Interaction Between Macromolecules*, Rocchia, W., Spagnuolo, M., Eds. *Cham, 2015* **2015**, 39–71.
- (18) Fenley, M. O.; Harris, R. C.; Mackoy, T.; Boschitsch, A. H. Features of CPB: A Poisson–Boltzmann solver that uses an adaptive cartesian grid. *J. Comput. Chem.* **2015**, *36*, 235–243.
- (19) Wang, C.; Wang, J.; Cai, Q.; Li, Z.; Zhao, H. K.; Luo, R. Exploring accurate Poisson–Boltzmann methods for biomolecular simulations. *Comput. Theor. Chem.* **2014**, *1:2*, 34–44.
- (20) Mirzadeh, M.; Theillard, M.; Gibou, F. A second-order discretization of the nonlinear Poisson–Boltzmann equation over irregular geometries using non-graded adaptive Cartesian grids. *J. Comput. Phys.* **2011**, *230*, 2125–2140.
- (21) Chen, D.; Chen, Z.; Chen, C.; Geng, W. H.; Wei, G. W. MIBPB: A software package for electrostatic analysis. *J. Comput. Chem.* **2011**, *32*, 657 – 670.
- (22) Wang, B.; Nguyen, D. D.; Zhao, Z.; Cang, Z.; Wei, G.-W. MIBPB: An accurate and reliable software package for electrostatic analysis. *Preprint* **2015**,
- (23) Richards, F. M. Areas, Volumes, Packing, and Protein Structure. *Annual Review of Biophysics and Bioengineering* **1977**, *6*, 151–176.
- (24) Connolly, M. L. Analytical molecular surface calculation. *Journal of Applied Crystallography* **1983**, *16*, 548–558.

- (25) Sanner, M. F.; Olson, A. J.; Spohner, J. C. Reduced surface: An efficient way to compute molecular surfaces. *Biopolymers* **1996**, *38*, 305–320.
- (26) Zhou, Y. C.; Wei, G. W. On the fictitious-domain and interpolation formulations of the matched interface and boundary (MIB) method. *J. Comput. Phys.* **2006**, *219*, 228–246.
- (27) Zhou, Y. C.; Zhao, S.; Feig, M.; Wei, G. W. High order matched interface and boundary method for elliptic equations with discontinuous coefficients and singular sources. *J. Comput. Phys.* **2006**, *213*, 1–30.
- (28) Yu, S. N.; Geng, W. H.; Wei, G. W. Treatment of geometric singularities in implicit solvent models. *Journal of Chemical Physics* **2007**, *126*, 244108.
- (29) Yu, S. N.; Zhou, Y. C.; Wei, G. W. Matched interface and boundary (MIB) method for elliptic problems with sharp-edged interfaces. *J. Comput. Phys.* **2007**, *224*, 729–756.
- (30) Yu, S. N.; Wei, G. W. Three-dimensional matched interface and boundary (MIB) method for treating geometric singularities. *J. Comput. Phys.* **2007**, *227*, 602–632.
- (31) Xia, K. L.; Zhan, M.; Wei, G. W. MIB Galerkin method for elliptic interface problems. *Journal of Computational and Applied Mathematics* **2014**, *272*, 195–220.
- (32) Geng, W.; Yu, S.; Wei, G. W. Treatment of charge singularities in implicit solvent models. *Journal of Chemical Physics* **2007**, *127*, 114106.
- (33) Decherchi, S.; Rocchia, W. A general and robust ray-casting-based algorithm for triangulating surfaces at the nanoscale. *PLoS ONE* **2013**, *8*, e59744.
- (34) Liu, B.; Wang, B.; Zhao, R.; Tong, Y.; Wei, G. W. ESES: software for Eulerian solvent excluded surface. *Preprint* **2015**,
- (35) Harris, R. C.; Bredenbergh, J. H.; Silalahi, A. R. J.; Boschitsch, A. H.; Fenley, M. O. Understanding the physical basis of the salt dependence of the electrostatic binding free energy of mutated charged ligand-nucleic acid complexes. *Biophysical Chemistry* **2011**, *156*, 79–87.

- (36) Pettersen, E. F.; Goddard, T. D.; Huang, C. C.; Couch, G. S.; Greenblatt, D. M.; Meng, E. C.; Ferrin, T. E. UCSF Chimera—a visualization system for exploratory research and analysis. *J. Comput. Chem.* **2004**, *25*, 1605–1612.
- (37) Feig, M.; Onufriev, A.; Lee, M. S.; Im, W.; Case, D. A.; Brooks, I., C. L. Performance comparison of generalized Born and Poisson methods in the calculation of electrostatic solvation energies for protein structures. *Journal of Computational Chemistry* **2004**, *25*, 265–284.
- (38) Reyes, C. M.; Kollman, P. A. Structure and thermodynamics of RNA-protein binding: using molecular dynamics and free energy analyses to calculate the free energies of binding and conformational change. *Journal of molecular biology* **2000**, *297*, 1145–1158.
- (39) Nicholls, A.; Mobley, D. L.; Guthrie, J. P.; Chodera, J. D.; Bayly, C. I.; Cooper, M. D.; Pande, V. S. Predicting small-molecule solvation free energies: an informal blind test for computational chemistry. *Journal of Medicinal Chemistry* **2008**, *51*, 769–779.
- (40) Shivakumar, D.; Williams, J.; Wu, Y.; Damm, W.; Shelley, J.; Sherman, W. Prediction of absolute solvation free energies using molecular dynamics free energy perturbation and the OPLS force field. *Journal of Chemical Theory and Computation* **2010**, *6*, 1509–1519.

